

Effect of droplet transfer mode on composition homogeneity of twin-wire plasma arc additively manufactured titanium aluminide

Jianwen Xin (✉ xinjianwen@sjtu.edu.cn)

Shanghai Jiao Tong University <https://orcid.org/0000-0001-5431-4070>

Dongsheng Wu

Haiyao Chen

Lin Wang

Wenlu Zhou

Kanglong Wu

Yuelong Zhang

Chen Shen

Xueming Hua

Fang Li

Research Article

Keywords: wire arc additive manufacturing, titanium aluminide, droplet transfer, composition homogeneity

Posted Date: July 26th, 2022

DOI: <https://doi.org/10.21203/rs.3.rs-1850325/v1>

License: © ⓘ This work is licensed under a Creative Commons Attribution 4.0 International License.

[Read Full License](#)

Abstract

Twin-wire plasma arc additive manufacturing (TW-PAAM) is an innovative process for titanium aluminide manufacture which is low in equipment cost and high in efficiency. However, as an in-situ alloying process, the composition homogeneity is typically a source of concern. The present work investigates this subject by observing the element input mode at various welding wire positions with a high-speed camera system and particle tracking method. It is found that when the welding wires are in a high position, the droplet enters the molten pool from the tip of the titanium wire, and the alloy element input interval is long, resulting in the formation of bands with high aluminium content at the edge of the deposition layer. When the welding wires are close to the workpiece surface, the droplet transfer mode switches to a mixture of dual wire-bridge transfer and Ti wire-bridge transfer. The diameter and transfer interval of the droplets decrease, as well as the heterogeneity of the deposition layer. The conclusion establishes a correlation between droplet transfer mode and composition homogeneity, which is beneficial for optimizing the TW-PAAM titanium aluminide fabrication process.

1 Introduction

With its high specific strength and excellent mechanical properties at high temperatures, γ -TiAl alloy is considered as an appropriate material for low pressure turbines of aeroengines. However, its intrinsic brittleness restricts the fabrication and shape-forming process using conventional casting techniques[1, 2]. Additive manufacturing, a method of layer-by-layer accumulation, has vast potential in the realm of precision production. Wire-Arc additive manufacturing (WAAM), compared with using electron beam or laser sources, has low equipment investment, low material cost and high manufacturing efficiency, making it a trend to be applied into γ -TiAl alloy manufacturing [3, 4, 5].

Unlike other WAAM deposition techniques, which always use a single welding wire to form the accumulation layer, twin wire-wire arc additive manufacturing, using two types of wires to melt into the molten pool respectively, and mixing in the molten pool to obtain the required alloy, has achieved progresses in titanium aluminide fabrication. Ma Y. et al.[6, 7], from University of Wollongong, were the first to employ this method to manufacture titanium aluminide, and studied the microstructure changes in the deposition layer caused by different thermal cycling conditions. Wang J. et al. [8] investigated the phase composition of titanium aluminide fabrication through adjusting the elemental wire feed rates. Using plasma arc as a heat source, Wang L. et.al[9, 10] from Shanghai Jiao Tong University established TW-PAAM method, increased the production efficiency and was able to accumulate titanium aluminide wall with the designed composition, and found that Ti-48Al has the best comprehensive mechanical properties. However, as an in-situ alloying process, the composition homogeneity is often a cause for concern. It is well known that these two metals have very different physical properties and are hard to combine with each other [11]. Titanium has a higher melting point of 1930 K than aluminium which is 930 K. In addition, the thermal conductivity of titanium is only $21.9 \text{ W} / (\text{m} \cdot \text{K})$, whereas that of aluminium is $237 \text{ W} / (\text{m} \cdot \text{K})$. Therefore, given the same heat source circumstances, aluminium wire will melt more quickly than titanium wire, making it far more difficult to send Al element into the molten pool.

In addition, in order to achieve a specific composition ratio, such as Ti-48Al, the wire feeding rate of the two wires must be predetermined and cannot be adjusted based on the disparity in melting speed of two wires. Therefore, numerous efforts have been expended to ensure the wires melt synchronously. Henckell et al.[12] used the titanium wire as anode of GMAW, and aluminium wire was fed from the side, which made it possible to adjust the wire feeding speed to coordinate with different composition of titanium aluminium alloy, but caused a relatively serious problem of uneven Ti-Al mixing. CAI et al.[13] used the "TOP-TIG" method to send the aluminium wire from the rear of the arc, which reduced the heat input of the aluminium wire, so that the aluminium can enter the molten pool stably, but the risk of composition heterogeneity was increased.

On the other hand, the vast disparities on density and surface tension between the two metals [14, 15] throw the homogeneity of the mixture into doubt in itself, as it is typically difficult for dissimilar metals to spontaneously mix uniformly. In cases conducted to other multicomponent systems, Zhang Q. et al.[16] used ER5183 welding wire with high magnesium content to weld on AA6063 aluminium alloy, and found that the macroscopic distribution of magnesium content was significantly deviating from the uniform under the influence of flow in the molten pool. Shamsolhodaie et al. [17] studied the element distribution in the laser welding process of nickel-copper butt joint and found that changing the laser beam position would alter the temperature distribution of the molten pool, leading to the macro heterogeneity of cuprum. Dong et al.[18] used WAAM method to produce α -CuAl alloy, and found that due to the great variance of thermal conductivity of Cu and Al, the intermetallic compounds CuAl_2 and Cu_9Al_4 phases appeared in the alloy wall. In laser or electron beam additive manufacturing of titanium aluminides, there is also the element heterogeneity problem of aluminium evaporation, caused by high molten pool temperature [19, 20]. In WAAM of titanium aluminide, the lower molten pool temperature is hard to cause aluminium lost. Therefore, wire melting and droplet transfer mode, and flow state in the molten pool can be defined as main factors of the uneven mixing problem of titanium and aluminium elements.

In the past, researchers have examined the melting and transfer phenomena of filling wires in gas tungsten arc welding and other welding forms. Taguchi et al [21] categorized transfer modes into four types based on the duration of droplet growth stage and droplet transfer stage. Rios S. et.al. [22] identified the droplet transfer modes in single filling wire plasma arc additive manufacturing based on Taguchi's work. Chen S. et al. [23] found that the droplet transfer mode could be altered by increasing power of the arc or wire spatial height. Huang J. et al. [24] discovered that for different droplet transfer modes, there are differences in the drop transfer interval, the diameter and mass of a single droplet, and the morphology after falling into the molten pool, thus would affect the flow of the molten pool through X-ray method. And in our further research [25], it is found that for the titanium aluminide additive manufacturing, the surface tension effect makes the droplet difficult to transfer easily, and the two welding wires interact to form new transfer modes. Consequently, in the case of TW-PAAM fabrication of titanium aluminide, the composition homogeneity of the additive alloy can be improved through elucidating the interaction between wire feeding and droplet transfer.

In the present work, the spatial height of the two welding wires is selected as the variables to alter the droplet transfer mode, thus the melting process of two welding wires and the molten pool flow state are analysed by high-speed video camera and tracing particle method. The relationship of element homogeneity in deposition layer and different transfer modes is confirmed by scanning electron microscope, which points out a direction for theoretical research and process optimization of titanium aluminide additive fabrication.

2 Experiment Procedures

A group of single layer single pass γ -TiAl welds were deposited on pure titanium plate utilizing plasma arc as heat source, with fixed welding current and wire feeding speed, and variable spatial height of wires (H). Although the problem of mixing homogeneity is raised based on titanium aluminide multilayer fabrication, single layer analysis preserves the main factors: wire melting, droplet transfer, and flow in the molten pool, while excluding the influence of re-melting in multilayers at this time. The pure titanium substrate may have a dilution effect on the element ration in the first deposition layer, but for the mixing process in the molten pool, the substrate only serves as a Ti mass source, and has little effect on other driving forces and flow state; therefore, it will not impede element homogeneity research.

The schematic drawing of TW-PAAM titanium aluminide is shown in Fig. 1. Pure Ar (99.8%) was utilized as plasma gas and shielding gas in the plasma arc section. To prevent the deposited layer from getting oxidized, a specially developed shielding device was used. The deposition substrate was a 6-mm-thick titanium plate that was placed on a heating platform and heated to 873K to prevent microcracks. Ti (TA2) and Al (ER1100) wires were fed in front of the plasma arc from both sides in the wire feeding section. The wire feeding speed of two wires was determined to be 130 cm/min for titanium wire and 115 cm/min for aluminium wire in order to obtain γ -TiAl with an element content ratio of 52:48(Ti-48Al).

The distance between the plasma torch and the substrate was maintained at 12 mm throughout the investigation. Along the welding direction, the two wires were arranged in a mirrorlike pattern, with a distance of 2 mm between the welding wire intersection and the center of the arc, the spatial height of wires (H), and an angle of 60° between the projection lines of the two wires on the workpiece plane and a 25° angle between the wires and the workpiece plane. Two experimental groups were done with H set at 3 mm and 5 mm. Additional TW-PAAM parameters are detailed in Table 1.

Table.1 Detailed TA-PAAM parameters

Parameters Values	
Current	120 A
Voltage	21 V
Deposition speed	5.4 cm/min
Protecting gas flow rate	10 L/min
Plasma gas flow rate	0.3 L/min
Shielding gas rate (in shielding device)	35 L/min
Wire diameter	0.8 mm
Electrode diameter	4.8 mm
Electrode tip angle	30°
Electrode setback	3.5 mm
Constricting nozzle diameter	4 mm

For studying the droplet process, a high-speed camera equipped with a narrowband filter with a wavelength of $640 \pm 6\text{nm}$ was used, with illumination provided by a Cavilux background laser lighting system of $640 \pm 10\text{nm}$. SiC tracing particles were employed to coat the substrate in the moving direction of the molten pool. By observing the path of the tracing particles in the molten pool, the influence of different transfer modes on the molten flow was analysed. The temperature data around the droplet was captured using an InfRec R500 infrared camera. In order to study the composition homogeneity, in addition to the conventional observation of metallographic specimens of the cross section of the weld, the longitudinal section on both sides of the weld was also selected for metallographic observation (the etchant was mixture solution of $\text{HF}:\text{HNO}_3:\text{H}_2\text{O} = 1:1:10$, using ZEISS Axio Imager A2m for OM) and SEM characterization (using NOVA Nano 230 field emission gun scanning electron microscope at 20 kV acceleration voltage, provided by Shanghai Jiao Tong University instrument analysis center).

3 Experiment Results

3.1 Droplet transfer modes

The examinations are conducted in two wire spatial height groups ($H = 3\text{mm}$ and $H = 5\text{mm}$). According to high-speed videos, it is found that there are two mainly transfer modes of TiAl TW-PAAM, which is consistent with our previous research. Moreover, when the wire spatial height varies, the primary droplet transfer modes also vary.

Taken the 3 mm group as an example, as depicted in Fig. 2, the first transfer mode is that the droplet hanging at the end of the Ti wire, gradually grows up through Al wire sending until the droplet contacts

with the molten pool (at 490 ms), and the droplets break away from the welding wire, enter the molten pool in a very short time to complete the transfer (at 510ms). This transfer mode is referred to “Ti wire-bridge mode” (Mode 1) in this paper. The second transfer mode is that the droplet grows up at the tip of the two wires (at 726 ms), forming a Ti-Al bridge, and is continuously sent into the molten pool while the liquid Ti-Al bridge kept connection (at 824 ms). This transfer mode is called “dual wires-bridge mode” (Mode 2). In the $H = 3$ mm experiments, the two transfer modes coexist. After numerous Ti wire-bridge mode droplet transfer, the droplet switches to dual wires-bridge mode and then back. However, in the $H = 5$ mm experiment, there is only “Ti wire-bridge mode”. Moreover, compared to the $H = 3$ mm experiment, the droplet growth stage is longer (from 0 ms to 1406 ms, in Fig. 3) and the droplet diameter increases.

Given the description of two transfer modes, let's back to the relationship of wire spatial heights and transfer modes. Because of the high surface tension, it is difficult for TiAl droplet to drop into molten pool in free transfer under gravity action. Therefore, the way the droplet entered the pool is obviously related to the height of the wire. As shown in Fig. 4, when H is raised to 5 mm, the droplet has ample area to grow up, and its average diameter expands to 4.2 mm. Then the droplet contacts with the molten pool, and a large amount of liquid metal rapidly enter into the molten pool in a very short time, generating Ti wire-bridge mode with a lengthy growth time and a short transfer time. When the spatial height of welding wire is 3mm, the transfer mode belongs to the intermediate state of Ti wire-bridge mode and dual wires-bridge mode, and the two modes occurs alternately, so as the droplet position. The average droplet growth time in the Ti wire-bridge mode is 815 ms at $H = 3$ mm, while the average transfer time is only 10 ms. However, in the dual wires-bridge mode, the weld material transfer is stable, the liquid Ti-Al bridge could maintain connection for up to 80 ms at $H = 3$ mm, and the average growth time is just 189 ms. When $H = 5$ mm, the droplet growing time is increased to 1838 ms, and the transfer time is also extended to 18 ms due to the larger droplet diameter.

3.2 Metallographically image and SEM images

When the transfer mode changes, the element homogeneity has corresponding changes. The samples are cut and prepared as Fig. 5(A). Figure 5(B)&(C) shows different sections of welds at different wires height. The majority of 3mm and 5mm welds are made up of matrix phases, but there are numerous parallel and widely spaced dark band at the layer borders that extend angularly into the interior of the deposition layer, and are corroded more strongly by etchants.

In order to study the dark bands distribution characteristics, we obtained the metallography of the longitudinal section at the edge of the deposition layer. From the longitudinal section obtained from 3mm weld, it is found that such dark tissues are not appeared on the side near the aluminium wire (Fig. 5(B) (1)), but on the side near the titanium wire (Fig. 5(B)(2)). The dark bands appear every few millimeters and extend from the center of the weld to the outer surface of the weld against the welding direction. The longitudinal section metallography at the edge of 5 mm weld (Fig. 5(C)) show that the band is found on both the aluminium wire side and the titanium wire side, and the area of dark band is larger than that of 3mm metallography, which means that the element heterogeneity is more serious.

Electron microscopy is used to obtain the element content distribution of 3mm weld, as shown in Fig. 7, the Al content of the weld as a whole is about 42%, and in the dark band, at the position 500–700 μm of line scan (the blue line in Fig. 6(D)), the Al content is 45–50%, showing a phenomenon of Al-enrichment. The target composition for the manufacture of TiAl alloy is 52%Ti + 48%Al. As the substrate is pure Ti plate, it is reasonable to have a low aluminium content in the first weld, but the difference in aluminium content indicated that the elements are not evenly mixed in the deposition layer, which is not desirable.

3.3 the flow mode in molten pool

To further study the influence of different transfer modes on molten pool flow state, SiC tracing particles are used to observe the flow state in the molten pool. Figure 7 and Fig. 8 shows the moving path of the tracing particles on the molten pool surface during the transfer stage. It can be seen that in dual wires-bridge mode, the tracing particles move from the front part of the molten pool to the tail of the molten pool, with a total time of about 50ms and a generally fast flow speed, as Fig. 7(A) shown. Fastest flow rate of molten pool in central area can reach about 0.48 m/s (Fig. 7(C)). Then deceleration process occurred, but the overall flow rate is higher than 0.2 m/s. It means that in dual wires-bridge mode, in the transfer stage, wire is sent to molten pool continuously, the molten pool flows at high velocity, which is advantageous to a mixture of different metals in the molten pool. Figure 9 shows the Ti wire-bridge mode. A large droplet enters the molten pool in a short time. When the droplet have not completely entered the molten pool, the metal in the central area of the molten pool flows slowly and the flow rate is relatively stable, about 0.19 m/s (Fig. 8(B)). At the time of 10ms after transfer, droplet is completely sent into the molten pool, forms waves, pushes molten metals fast backward. The velocity of molten pool surface increased to 0.49 m/s, never stall until arriving at the molten pool tail area (Fig. 8(D)), indicating that at the transferal moment, the droplet has a strongly impingement effect. The flow and mixing effect would keep within a short period of time after transfer.

Figure 9 shows the flow state on the molten pool surface during growing stage (30ms after droplet transfer of both transfer modes respectively). After the welding wire is disconnected from the molten pool, the molten pool is in the state of self-flow in the two modes. The difference is that, in the dual wires-bridge mode, the droplet growing stage is shorter, often less than 100ms, while in the Ti wire-bridge mode, the droplet growth time could be as long as hundreds of milliseconds. In the stage of droplet growth and molten pool artesian flow, the flow velocity of molten pool surface slows down. At 40ms after the transfer, the surface velocity in the middle of the molten pool is still about 0.3m/s, but at 140ms after the transfer, the surface velocity in the middle of the molten pool is reduced to 0.09m/s, slowing down by 70%. The flow in the molten pool slows down and the overall mixing effect of the molten pool is affected. Therefore, the Ti wire-bridge mode is not conducive to uniform mixing for alloy elements in the molten pool.

4 Discussions

4.1 The relationship of two transfer mode

Although wire spatial height has been proved to be an effective factor in changing the droplet transfer pattern, the switching process of the two droplet transfer modes when the height of welding wire is 3mm can still provide some insights for TW-PAAM process. Figure 10 shows the temperature distribution around the droplet obtained by infrared camera under such conditions. In dual wires-bridge transfer (Fig. 10(A)), the TiAl bridge enters the arc center and is connected to the molten pool at a lower temperature of about 1670K; in Ti wire-bridge mode (Fig. 10(B)), the TiAl bridge (or droplet) is at a temperature of higher than 2200K. According to the qualitative calculation of surface tension data, $\gamma_{Ti} > \gamma_{TiAl} > \gamma_{Al}$, thus the wettability of liquid titanium aluminium on the surface of titanium wire is better than that on the surface of aluminium wire, so the liquid titanium aluminium bridge is produced by the continuous migration of liquid titanium aluminium alloy from aluminium wire to titanium wire, which has been described in our previous research [25]. However, the temperature coefficient of surface tension of liquid Ti-Al alloy is negative. When the temperature raised, the liquid bridge accelerated to separate from the aluminium wire, resulting in the fracture of Ti-Al liquid bridge.

Furthermore, there are variances in melting velocity among distinct droplet transfer modes, according to statistics acquired from high-speed photography. The theoretical melting velocity of the wires should be equal to the wire feeding rate once the droplet transfer has reached a steady state. The volume of melting or feeding per second is utilized as the unit of melting velocity in this study since two single metal wires are used, and the volume change after the two metal melts mixing is neglected.

$$v_0 = v_{Al} \times S_{Al} + v_{Ti} \times S_{Ti}$$

1

.....

The wire feeding parameters have been given above.

Sine the actual droplet transfer process is undergoing two stages: droplet growth and droplet entry into the molten pool, it cannot be approximated as a steady-state mode. As a result, the average volume of droplet entering the molten pool in each transfer is divided by the average interval of each transition to determine the average melting velocity of the wires.

$$v = \frac{(1 - \alpha) \times \frac{1}{6} \pi d^3}{T}$$

2

.....

where α is the percentage of droplets remaining at the tip of the wires after each transfer process, estimated as 10% in this study. And d is the diameter of the droplet at the moment of contacting the molten pool, T is the average transfer interval.

Table.2 melting velocity in different transfer mode

Transfer Mode	d (mm)	T (s)	v (mm^3/s)
Ti wire-bridge (H = 5 mm)	4.2	1.855	$v_1 = 18.81$
Ti wire-bridge (H = 3 mm)	2.5	0.824	$v_2 = 8.93$
Dual wires-bridge (H = 3 mm)	-	-	$v_3 \approx v_0 = 20.53$

The results are listed in Table.2. Thus, we find that in Ti wire-bridge transfer (H = 3 mm), the melting velocity(v_2), is slower than the wire feeding speed(v_0), so in this mode, the tip of wires is not easy to keep in the same position for droplet transfer, but often sent forward, to be more close to the arc and molten pool, and then switch to the dual wire-bridge transfer mode. In addition, according to the above surface tension analysis, after the wire is sent forward, titanium and aluminium mixture tend to move upward along the Ti wire due to the heat transfer change at the tip of the wire, which promotes the breakup of the titanium and aluminium liquid bridge. Therefore, the droplet transfer mode is changed to Ti wire-bridge transfer again. For H = 5mm, the actual melting velocity (v_1) matches the theoretical melting speed (v_0), the melting point position moves less, and the droplet transition process is stable. However, the large droplet size in this state tends to cause the problem of non-uniformity of composition.

4.2 The generation of aluminium nonuniformity

According to the experiment results, the Al-rich areas appear and expand with the wire spatial height is raised. The differences of microstructure are matched with the difference of droplet transfer mode, which indicated that droplet transfer is the main reason for the uneven mixing process. In the additive process, the pure titanium workpiece melted under the action of arc, and the matrix phase is lack of aluminium. As the welding wires are sent into the molten pool, all aluminium elements are supplied by the droplet, so it can be inferred that the aluminium-rich tissue is the residue of the droplet after entering the molten pool.

In order to understand how the difference in wire height leads to the generation of Al-rich band, we first need to discuss how H affects the mass transfer process of alloying elements. When the wire spatial height is low, the droplet stays in the arc high temperature zone for a short time, and contacts with the molten pool as soon as it forms. As the wire continues to be fed, alloying elements enter the molten pool in a continuous dual wire-bridge mode, promoting the continuous high-speed flow of the molten pool, and completing the mixing and homogenization process in the flow process. But when the wire height is high, the droplet will stay in the arc high temperature region for a long time. However, because of the high surface tension of Ti, the droplet will be suspended at the end of the Ti wire. When the Al wire is sent in,

the Al element will enter the droplet, and the droplet continue to grow, but it is difficult to mix evenly in the droplet. Until the droplet grows to contact with the surface of the molten pool, a large number of unevenly mixed metal melts enter the pool in a short time and are remixed in the flow process of the pool.

Figure 11 concluded the formation process of Al element nonuniformity. Under the influence of Marangoni effect, liquid metal flows outwards on the cross section of molten pool, and under the influence of arc pressure, shear force, buoyancy and other factors, liquid metal flows to the rear of molten pool. The area near the arc center is affected by arc pressure and mainly flows downward. Therefore, the surface flow of molten pool is mainly backward along the edge of molten pool (Fig. 11(A)). When the droplet enters the molten pool, there is an impingement effect on the molten pool, and a large amount of liquid metal that is not completely mixed enters the molten pool, which pushes the liquid metal in the molten pool to flow backward rapidly and aggregate in the rear. Under the influence of arc pressure and shear force, these unmixed liquid metals are difficult to be distributed evenly in the molten pool by convection, and can only accumulate at the edge of the molten pool under the influence of Marangoni effect, thus forming the Al-rich band (Fig. 11(B)).

There is also evidence that showed correlation between transfer mode and the composition homogeneity. In the Ti wire-bridge mode, the droplet transfer period is about 1 to 2 seconds, while the welding speed is 0.9 mm/s, so the workpiece moved forward 0.9 to 1.8 mm, which is the same order of magnitude as the Al-rich band. In addition, under the condition of 5 mm wire height, the droplet growth time is longer, the droplet average diameter is larger, after falling into the molten pool, compared with 3mm weld, so there are more aluminium rich liquid groups, forming aluminium rich band after solidification, deservedly. In summary, it could be inferred that the uneven mixing phenomenon is caused by the Ti wire-bridge mode.

5 Conclusion

A) There are two transfer modes in TW-PAAM titanium aluminide process: dual wires-bridge mode and Ti wire-bridge mode. With the increase of wire height, droplet transfer mode changes from dual wires-bridge mode to Ti wire-bridge mode.

B) In the two droplet transfer modes, the dual wires-bridge transfer has a long-term acceleration effect on the molten pool. However, in the Ti wire-bridge mode, the droplet growth time is longer and the transfer time is shorter. Although its big droplet has impact and agitation effect on the molten pool, the molten pool movement speed would decrease in the growth stage, which is not conducive to the uniform mixing of alloy elements.

C) The distribution of alloying elements in the molten pool undergoes the process from non-uniform to uniform during the manufacturing of TiAl alloy by TW-PAAM. In the Ti wire-bridge mode, when droplets enter into the molten pool, Al-rich drops move toward the tail of molten pool, and form Al-rich bands on both sides of deposition layer. The areas and interval of Al-rich bands are positively correlated with droplet diameter and transfer interval. Therefore, Ti wire-bridge mode is not an ideal method for TW-PAAM TiAl alloy.

Declarations

Funding

This research is partially supported by both the Science and Technology Commission of Shanghai Municipality (STCSM, Funding No. 19511106400, "Sailing Program" No. 19YF1422700) and the "JSPS International Research Fellow" project (21F31063).

Competing Interests

The authors have no relevant financial or non-financial interests to disclose.

Author Contributions

All authors contributed to the study conception and design. Material preparation, data collection and analysis were performed by Xin Jianwen and Chen Haiyao. The first draft of the manuscript was written by Xin Jianwen and all authors commented on previous versions of the manuscript. All authors read and approved the final manuscript.

References

1. Wu Xinhua. 2006. Review of alloy and process development of TiAl alloys, *Intermetallics*, 14(10), 1114-1122. <https://doi.org/10.1016/j.intermet.2005.10.019>
2. Zhang, X., Chen, Y., Hu, J., 2018. Recent advances in the development of aerospace materials. *Progress in Aerospace Sciences*, 97: 22-34. <https://doi.org/10.1016/j.paerosci.2018.01.001>
3. Wu, B., Pan, Z., Ding, D., et al., 2018. A review of the wire arc additive manufacturing of metals: properties, defects and quality improvement. *Journal of Manufacturing Processes*, 35, 127-139. <https://doi.org/10.1016/j.jmapro.2018.08.001>
4. Debroy, T., Wei, H.L., Zuback J.S., et al., 2018. Additive manufacturing of metallic components - Process, structure and properties. *Progress in Materials Science*, 92, 112-224. <https://doi.org/10.1016/j.pmatsci.2017.10.001>
5. Emiralioğlu, A., Ünal, R. 2022. Additive manufacturing of gamma titanium aluminide alloys: a review. *Journal of Materials Science*, 57, 4441–4466. <https://doi.org/10.1007/s10853-022-06896-4>
6. Ma, Y., Cuiuri, D., Hoye, N., et al., 2014. Effects of wire feed conditions on in situ alloying and additive layer manufacturing of titanium aluminides using gas tungsten arc welding. *Journal of Materials Research*, 29(17), 2066-2071. <https://doi.org/10.1557/jmr.2014.203>
7. Ma, Y., Cuiuri, D., Hoye, N., et al., 2015. The effect of location on the microstructure and mechanical properties of titanium aluminides produced by additive layer manufacturing using in-situ alloying and gas tungsten arc welding. *Materials Science and Engineering A*, 631, 230-240. <https://doi.org/10.1016/j.msea.2015.02.051>

8. Wang, J., Pan, Z., Cuiuri, D., et al., 2019. Phase constituent control and correlated properties of titanium aluminide intermetallic alloys through dual-wire arc additive manufacturing. *Materials Letters*, 242, 111-114. <https://doi.org/10.1016/j.matlet.2019.01.112>
9. Wang, L., Shen, C., Zhang, Y., et al., 2021. Effect of Al content on the microstructure and mechanical properties of gamma-TiAl alloy fabricated by twin-wire plasma arc additive manufacturing system. *Materials Science and Engineering A*, 826, 142008-. <https://doi.org/10.1016/j.msea.2021.142008>
10. Wang, L., Zhang, Y., Hua, X., et al., 2021. Fabrication of γ -TiAl intermetallic alloy using the twin-wire plasma arc additive manufacturing process: Microstructure evolution and mechanical properties. *Materials Science and Engineering A*, 812, 141056-. <https://doi.org/10.1016/j.msea.2021.141056>
11. Gadakh, V.S., Badheka, V.J., Mulay A.S., 2021. Solid-state joining of aluminium to titanium: A review [J]. *Proceedings of the Institution of Mechanical Engineers Part L*, 235(8), 1757-1799. <https://doi.org/10.1177/14644207211010839>
12. Henckell, P, Ali, Y., Metz, A., et al., 2019. In situ production of titanium aluminides during wire arc additive manufacturing with hot-wire assisted GMAW process. *Metals*, 9(5), 578. <https://doi.org/10.3390/met9050578>
13. Cai, X., Dong B., Yin X., et al., 2020. Wire arc additive manufacturing of titanium aluminide alloys using two-wire TOP-TIG welding: Processing, microstructures, and mechanical properties. *Additive Manufacturing*, 35,101344-. <https://doi.org/10.1016/j.addma.2020.101344>
14. Duan, S-C., Guo, H-J., 2020. Determination of viscosity and surface tension of liquid Ni–Al–Ti system using the evaluated thermodynamic properties by AMCT. *Journal of Materials Science*, 55(25), 11071-11085. <https://doi.org/10.1007/s10853-020-04841-x>
15. Liu, X., Lv, X., Li, C., et al., 2017. Surface tension of liquid Ti-Al alloys. *Rare Metal Materials and Engineering*, 46(1): 39-44, [https://doi.org/10.1016/S1875-5372\(17\)30074-7](https://doi.org/10.1016/S1875-5372(17)30074-7)
16. Zhang, Q., Dong, Q., Wang, X., et al. 2020. Predictions of solute mixing in a weld pool and macro-segregation formation during dissimilar-filler welding of aluminium alloys: Modelling and experiments. *Journal of Materials Research and Technology*, 9(6), 12080-12090. <https://doi.org/10.1016/j.jmrt.2020.08.109>
17. Shamsolhodaie, A., Sun, Q., Wang, X., et al. 2020. Effect of laser positioning on the microstructure and properties of niti-copper dissimilar laser welds. *Journal of Materials Engineering and Performance*, 29(2), 849-857. <https://doi.org/10.1007/s11665-020-04637-9>
18. Dong, B., Pan, Z., Shen, C., et al., 2017. Fabrication of copper-rich cu-al alloy using the wire-arc additive manufacturing process. *Metallurgical and Materials Transactions B*, 48(6), 3143-3151. <https://doi.org/10.1007/s11663-017-1071-0>
19. Schwerdtfeger, J., Körner, C., 2014. Selective electron beam melting of Ti–48Al–2Nb–2Cr: microstructure and aluminium loss. *Intermetallics*, 49: 29-35. <https://doi.org/10.1016/j.intermet.2014.01.004>
20. Gussone, J., Hagedorn, Y-C., Gherekhloo, H., et al., 2015. Microstructure of γ -titanium aluminide processed by selective laser melting at elevated temperatures. *Intermetallics*, 66: 133-140.

<https://doi.org/10.1016/j.intermet.2015.07.005>

21. Taguchi, H., Haneda, M., Imanaga, S., et al., 1979. Metal transfer in plasma arc. Journal of the Japan Welding Society, 48(7), 488-493. <https://doi.org/10.2207/qjjws1943.48.488>
22. Ríos, S., Colegrove, P.A., Williams, S.W., 2019. Metal transfer modes in plasma wire + arc additive manufacture. Journal of Materials Processing Technology, 264, 45-54. <https://doi.org/10.1016/j.jmatprotec.2018.08.043>
23. Chen, S., Zhang, S., Huang, N., et al., 2016. Droplet transfer in arcing-wire GTAW. Journal of Manufacturing Processes, 23, 149-156. <https://doi.org/10.1016/j.jmapro.2016.05.014>
24. Huang, J., Li, Z., Yu, S., et al., 2021. Real-time observation and numerical simulation of the molten pool flow and mass transfer behavior during wire arc additive manufacturing. Welding in the world, 66, 481-494. <https://doi.org/10.1007/s40194-021-01214-z>
25. Xin, J., Wu, D., Shen, C., et al., 2022. Multi-physical modelling of alloy element transportation in wire arc additive manufacturing of a γ -TiAl alloy. International Journal of Thermal Sciences. 179,107641-. <https://doi.org/10.1016/j.ijthermalsci.2022.107641>

Figures

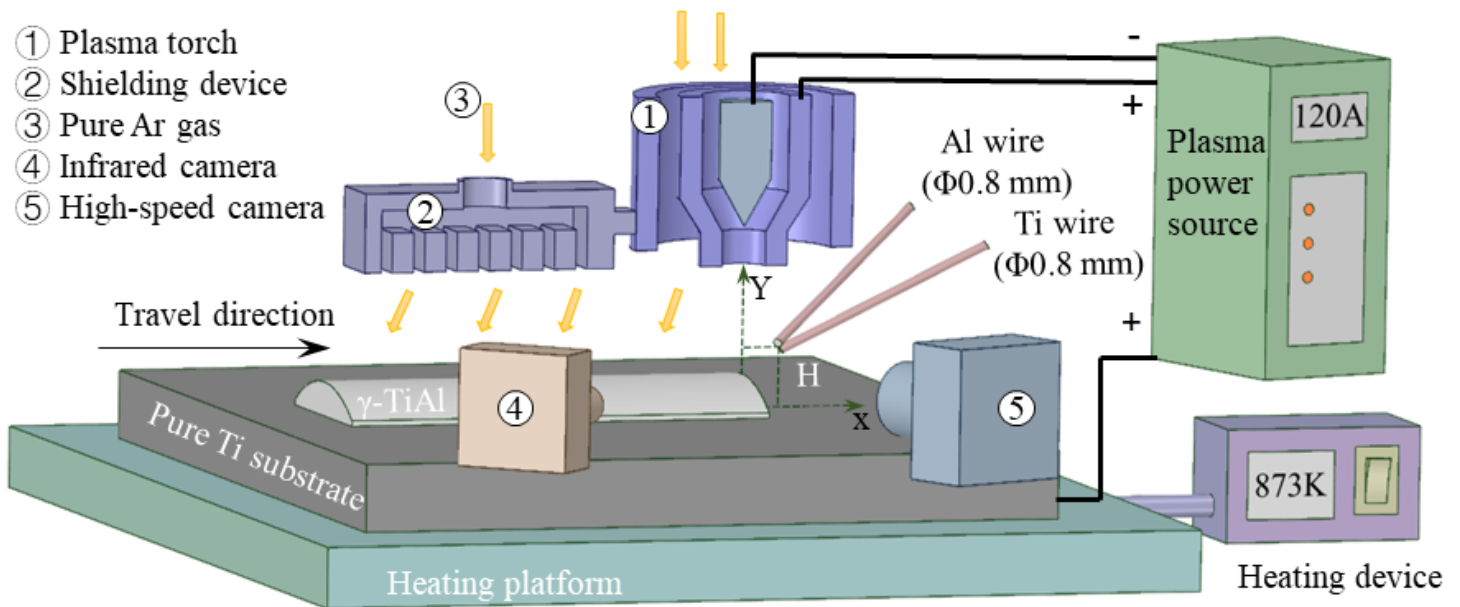


Figure 1

the Schematic diagram of TW-PAAM equipment

Figure 2

Droplet transfer process (H = 3 mm)

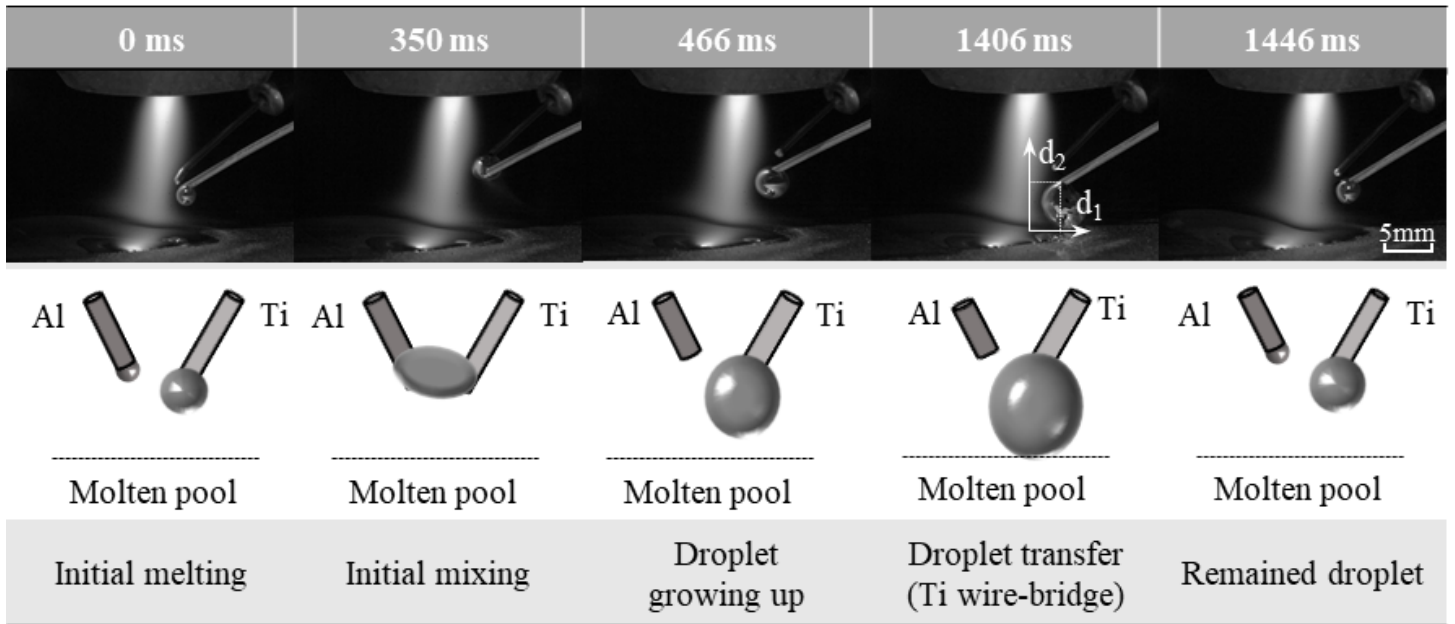


Figure 3

Droplet transfer process ($H = 5 \text{ mm}$)

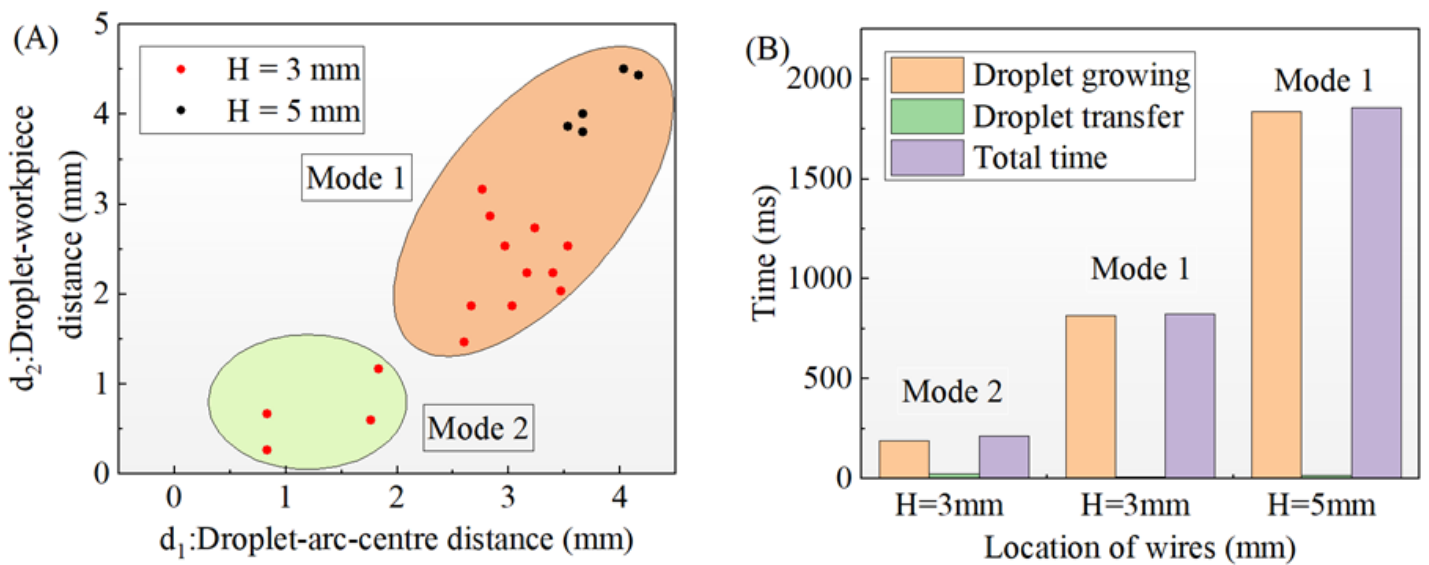


Figure 4

statistics of droplet transfer mode and the height of wires: (A) the location characteristic of droplet transfer mode;(B) the time characteristic of droplet transfer mode

Figure 5

metallographs of γ -TiAl (A) diagram of sample cutting;

(B) H = 3 mm (C) H = 5 mm; (1) Ti side (2) Al side

Figure 6

The SEM images of 3mm welds in the cross section (a) scanning position (b) Al distribution (c) Ti distribution (d) line distribution

Figure 7

Particle velocity during transfer stage, dual wires-bridge mode (H = 3mm)

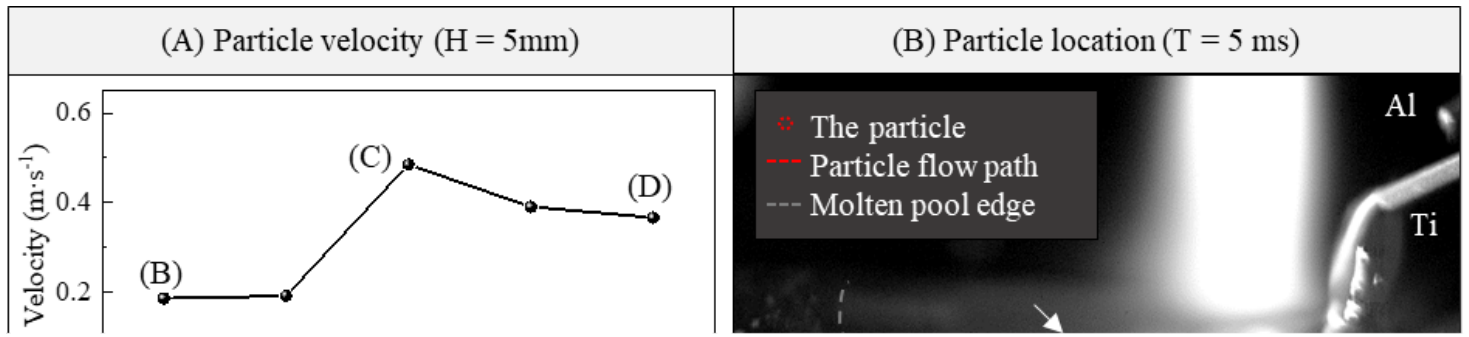


Figure 8

Particle velocity during transfer stage, Ti wire-bridge mode (H =5mm)

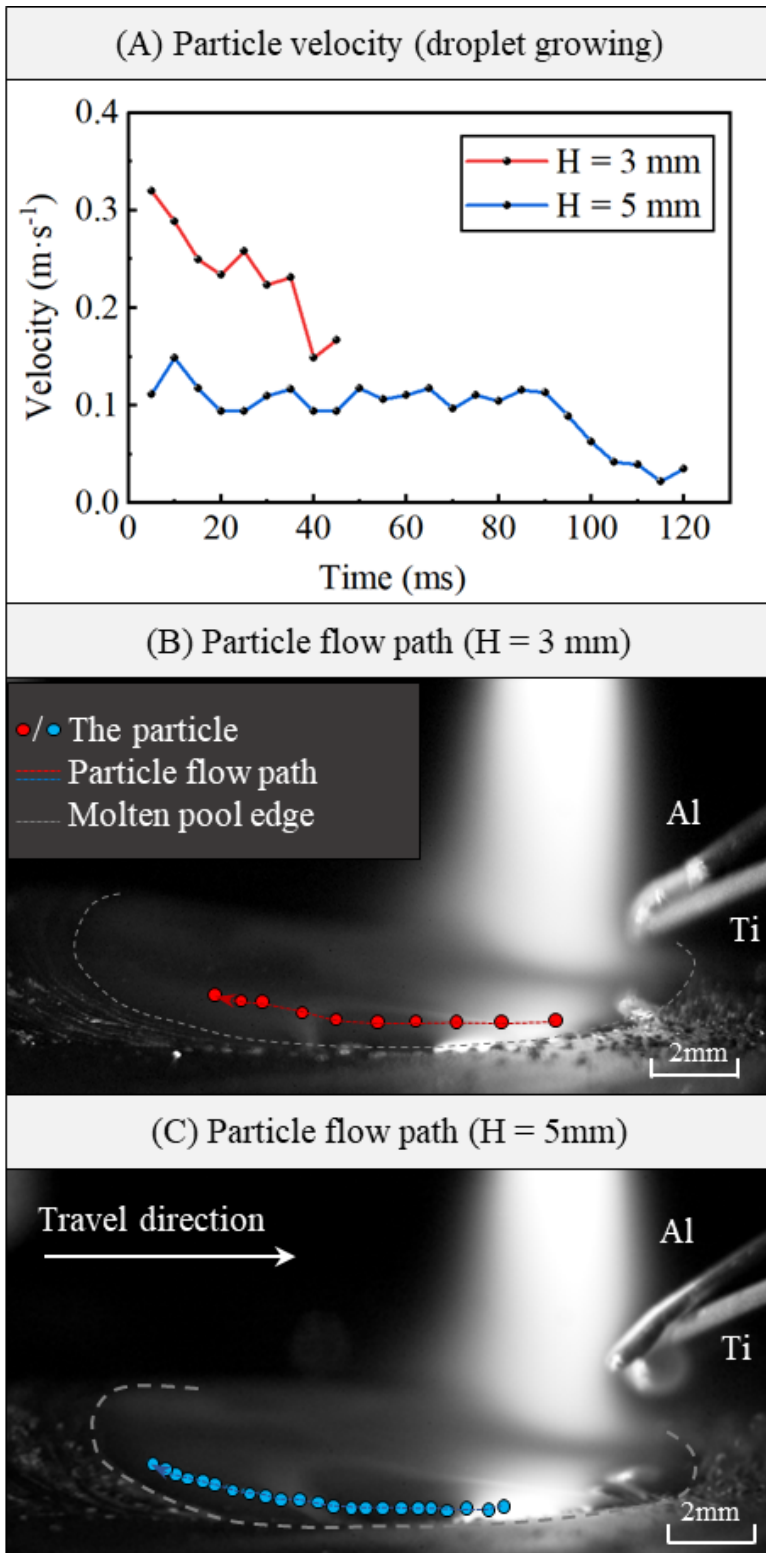


Figure 9

Particle velocity during growing stage

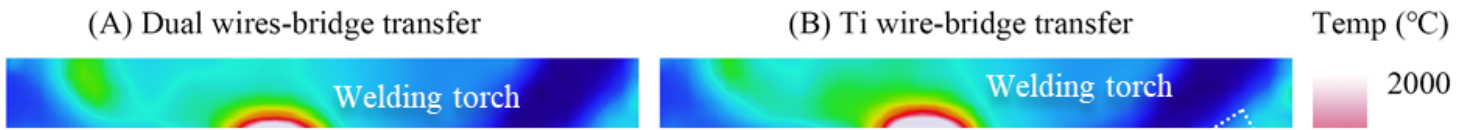


Figure 10

The temperature of droplet in different transfer modes (H=3 mm)

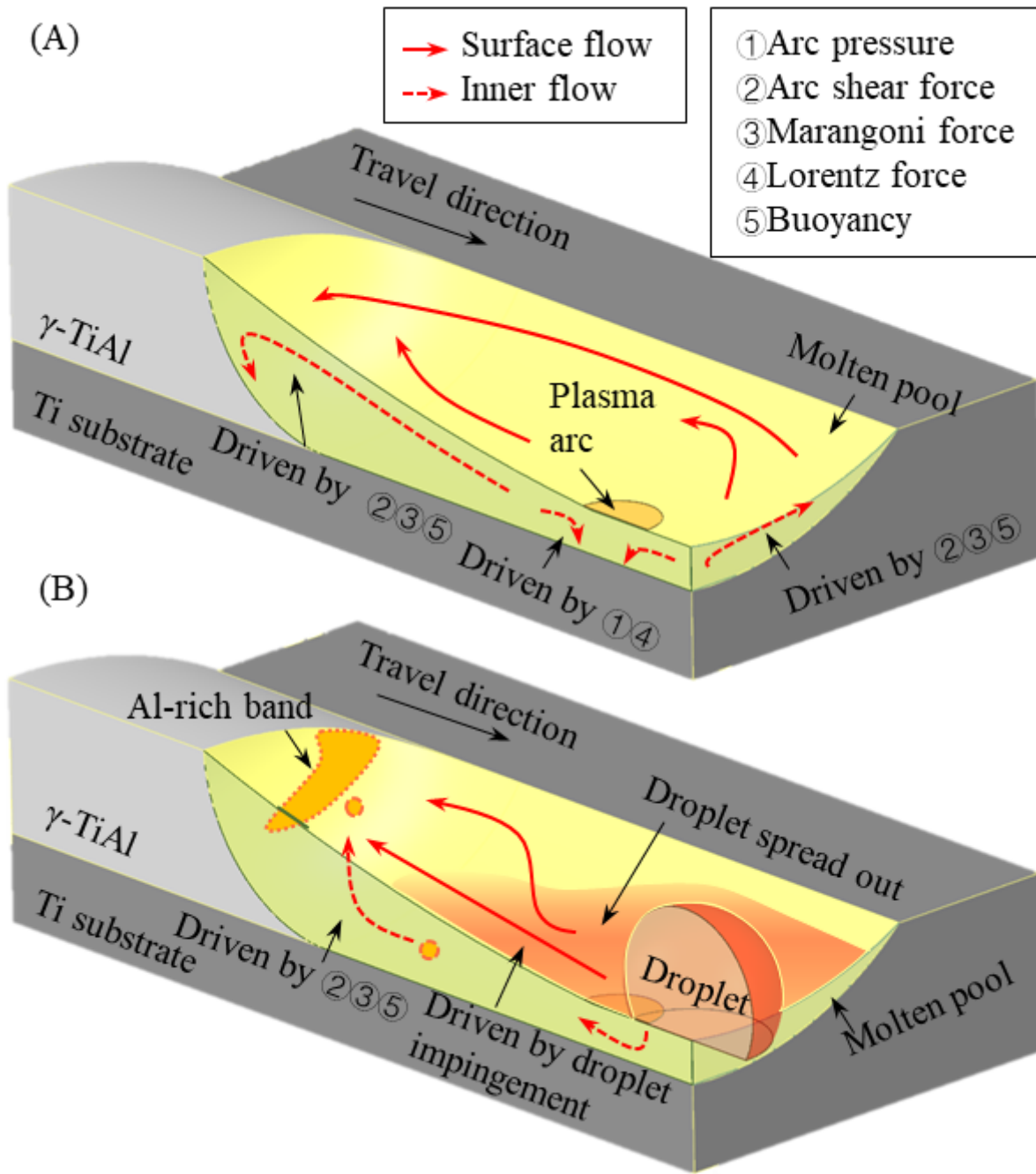


Figure 11

the formation of mixing nonuniformity (A) fluid flow mode and driven forces in the molten pool (B) the droplet impingement changes the flow and makes the Al-rich band